

# Saturation of Rogue Wave Amplification over Steep Shoals

Saulo Mendes <sup>1,2,\*</sup> and Jerome Kasparian <sup>1,2,†</sup>

<sup>1</sup>*Group of Applied Physics, University of Geneva,  
Rue de l'École de Médecine 20, 1205 Geneva,, Switzerland*

<sup>2</sup>*Institute for Environmental Sciences, University of Geneva,  
Boulevard Carl-Vogt 66, 1211 Geneva, Switzerland*

Shoaling surface gravity waves induce rogue wave formation. Though commonly reduced to water waves passing over a step, non-equilibrium physics allows finite slopes to be considered in this problem. Using non-homogeneous spectral analysis of a spatially varying energy density ratio we describe the dependence of the amplification as a function of the slope steepness. Increasing the slope increases the amplification of rogue wave probability, until this amplification saturates at steep slopes. In contrast, the increase of the down slope of a subsequent de-shoal zone leads to a monotonic decrease in the rogue wave probability, thus featuring a strong asymmetry between shoaling and de-shoaling zones. Due to the saturation of the rogue wave amplification at steep slopes, our model is applicable beyond its range of validity up to a step, thus elucidating why previous models based on a step could describe the physics of steep finite slopes. We also explain why the rogue wave probability increases over a shoal while it is lower in shallower water.

## I. INTRODUCTION

Rogue waves have been observed in a variety of fields of physics [1], such as astrophysics [2, 3], optics [4, 5] and condensed matter physics [6, 7]. In the ocean, they present a threat to ocean vessels and offshore operations [8, 9]. In the latter case, most studies have focused on deep water, where both Benjamin and Feir [10] instability and quasi-determinism theory [11] apply. The study of wave statistics evolving from deep toward shallow water regimes have become a recent trend. On the other hand, no standard distribution reproduces observations over a wide range of depths and sea states [12, 13]. For sea states in equilibrium (without shoaling), it may be possible to describe both deep and shallow regimes with second-order models of enhanced empirical parameter space (steepness, bandwidth, depth) [14, 15], albeit such methods lack first principles of the physical problem. For seas out of equilibrium, experiments in shallower regimes have shown that inhomogeneities in the wave field due to shoaling contribute to rogue wave formation and amplification [16–18]. Paradoxically, rogue waves are less likely to occur in shallow waters as compared to deep waters [19, 20]. Furthermore, spatial statistics for seas in both equilibrium and out-of-equilibrium are not captured by available theories [21, 22].

Recently, successful theories of rogue wave shoaling have arisen. For an abrupt bathymetry change, Li *et al.* [23, 24] propose a solution in terms of the transmission coefficients and the interaction of bound waves influenced by the step. On the other hand, Majda *et al.* [25] and Moore *et al.* [26] dealt with a step transition implementing a truncated KdV model. However, the homogeneity of surface waves is often assumed [27], whereas the relaxation of this condition is expected to play a role in rogue

wave formation over a shoal [28]. Indeed, we recently provided a third framework [29] by taking non-homogeneity into account. These three frameworks are complementary, because they rely on different physical approaches, respectively: fluid dynamics analysis of wave harmonics, the statistical mechanics of water waves, and the lifting of long-held implicit assumptions regarding the homogeneity of ocean waves. Nonetheless, the generality of the third framework may have the advantage of being applicable to any out-of-equilibrium water wave problem besides non-uniform bathymetry, such as opposing currents [30] or reflection [31].

Although the influence of the slope steepness on rogue wave enhancement over a shoal has been demonstrated in numerical simulations [32–34], none of the three approaches described above consider the effect of the slope steepness  $\nabla h(x) \equiv \partial h(x)/\partial x$  explicitly. Therefore, the current work addresses analytically the problem of how the slope affects the amplification of extreme events when irregular waves travel over a shoal. We show that the slope mainly decreases the spatial energy density and thus increases the non-homogeneous correction  $\Gamma$  introduced in Mendes *et al.* [29], increasing the rogue wave probability. Also, this slope effect saturates beyond a critical steepness. We thus provide a physical interpretation to the observation of this saturation by Zheng *et al.* [33]. Our theory explains why the physics of steep finite slopes can be well described by the three above theories. Furthermore, the slope effect saturates for mild slopes in shallow waters, explaining why it is important in intermediate depths, while dying out not only in deep water but paradoxically also in shallow waters.

## II. THEORETICAL CONSIDERATIONS

Rather than a deterministic approach based on the hydrodynamic description of the rogue wave evolution over a shoal, the model of Mendes *et al.* [29] uses a statis-

\* saulo.dasilvamendes@unige.ch

† jerome.kasparian@unige.ch

tical approach focused on the integral properties of the wave system [35], namely the energy density. It considers the perturbation induced by the shoal on the surface elevation and thus on the energy partition, which in turn affects the statistics of water waves. This perturbation is spatially inhomogeneous and thereby redistributes the wave energy density throughout the bathymetry change. To derive the corresponding correction  $\Gamma$  to the distribution capturing the energetic spatial evolution, we consider the velocity potential  $\Phi(x, z, t)$  and surface elevation  $\zeta(x, t)$ , written in generalized form of an expansion of trigonometric functions with coefficients  $(\Omega_{m,i}, \tilde{\Omega}_{m,i})$ :

$$\begin{aligned}\Phi(x, z, t) &= \sum_{m,i} \frac{\Omega_{m,i}(k_i h)}{m k_i} \cosh(m\varphi) \sin(m\phi) \quad , \\ \zeta(x, t) &= \sum_{m,i} \tilde{\Omega}_{m,i}(k_i h) \cos(m\phi) \quad ,\end{aligned}\quad (1)$$

with the auxiliary variables  $\varphi = k_i(z + h)$  and  $\phi = k_i(x - c_{m,i}t + \theta_i)$  where  $c_{m,i} = c_m(k_i)$  is the phase velocity of the  $i$ -th spectral component and  $m$ -th order in wave steepness and  $h$  the water depth. For unidirectional waves of first-order in steepness we extract  $\Omega_1 = a\omega/\sinh kh$  as well as  $\tilde{\Omega}_1 = a$  from linear theory [36], leading to the energy density [37]:

$$\mathcal{E} = \frac{1}{2} \rho g \sum_i a_i^2 \quad , \quad (2)$$

where  $\rho$  is the density,  $g$  is the gravitational acceleration,  $a$  is the wave amplitude. A spectral energy  $\mathcal{E}$  is preferred to match the definition of power in signal processing [38, 39], such that we define  $\mathcal{E} = \rho g \mathcal{E}$ . Due to the spatial inhomogeneity in  $\mathcal{E}$  and the ensemble average  $\mathbb{E}[\zeta^2]$ , an initially Rayleigh distribution over a flat bottom becomes  $\mathcal{R}_{\alpha,\Gamma}(H > \alpha H_s) = e^{-2\alpha^2/\Gamma}$ , where the non-homogeneous correction  $\Gamma$  is [29]:

$$\Gamma(x) = \frac{\mathbb{E}[\zeta^2(x, t)](x)}{\mathcal{E}(x)} \approx \frac{\langle \zeta^2(x, t) \rangle_t(x)}{\mathcal{E}(x)} \quad . \quad (3)$$

Second-order waves have energy density ratio [29]:

$$\tilde{\mathcal{E}}(x) \equiv \frac{2\mathcal{E}(x)}{a^2} = 1 + \frac{\pi^2 \varepsilon^2(x) \mathfrak{S}^2}{32} [\tilde{\chi}_1(x) + \chi_1(x)] \quad , \quad (4)$$

where  $\varepsilon = H_s/\lambda$  the significant steepness of irregular waves with the significant wave height  $H_s$  (the average height of the 1/3 tallest waves), zero-crossing wavelength  $\lambda$ , and with coefficients dependent on the peak wavenumber  $k_p = 2\pi/\lambda_p$ :

$$\tilde{\chi}_1 = \left[ \frac{3 - \tanh^2(k_p h)}{\tanh^3(k_p h)} \right]^2, \quad \chi_1 = \frac{9 \cosh(2k_p h)}{\sinh^6(k_p h)} \quad . \quad (5)$$

Moreover,  $1 \leq \mathfrak{S} \leq 2$  denotes the slowly varying vertical asymmetry between crests and wave heights ( $a = \mathfrak{S}H/2$ ), which for rogue waves reads [13, 29]:

$$\mathfrak{S}_{(\alpha=2)} \approx \frac{2\eta_s}{1 + \eta_s} \left( 1 + \frac{\eta_s}{6} \right), \quad \eta_s = \left( \frac{\langle \mathcal{Z}_c \rangle}{\langle \mathcal{Z}_t \rangle} \right)_{H > H_s} \quad , \quad (6)$$

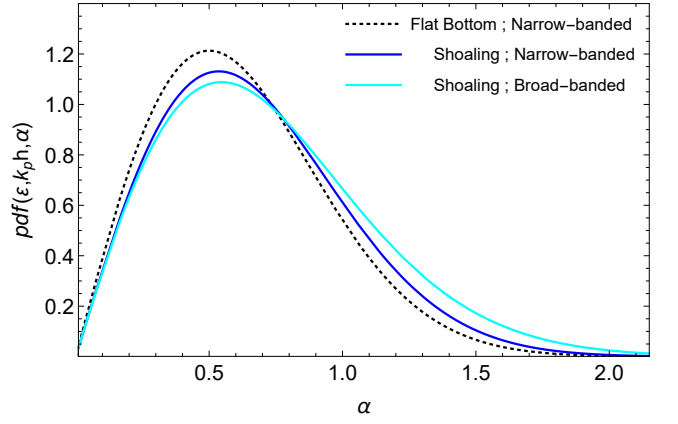


FIG. 1: Probability density due to energy density inhomogeneities caused by a shoal as compared to the Rayleigh distribution (dotted) for wave heights. Shoaling featured steepness  $\varepsilon = 1/20$  while broad-banded waves have  $\mathfrak{S}(\alpha = 2) = 1.20$  and narrow-banded  $\mathfrak{S}(\alpha = 2) = 1.05$  instead.

given the mean crest  $\langle \mathcal{Z}_c \rangle$  and mean trough  $\langle \mathcal{Z}_t \rangle$ . In the limit  $\varepsilon \rightarrow 0$  we recover  $\mathcal{E} = 1$  for linear waves. The physics of second-order waves leads to [40]:

$$\Gamma \equiv \Gamma(\varepsilon(x), k_p h(x), \mathfrak{S}(x)) = \frac{1 + \frac{\pi^2 \varepsilon^2 \mathfrak{S}^2}{16} \tilde{\chi}_1}{1 + \frac{\pi^2 \varepsilon^2 \mathfrak{S}^2}{32} (\tilde{\chi}_1 + \chi_1)} \quad . \quad (7)$$

From the point of view of the energy density, both a homogeneous energy density of steep waves ( $\varepsilon \sim 1/10$ ) over a flat bottom and a non-homogeneous energy density of very small waves ( $\varepsilon \ll 1/100$ ) over a shoal induce a Rayleigh distribution for wave heights [41]. Otherwise, the disparity in the growth of  $\mathbb{E}[\zeta^2(x, t)]$  and  $\mathcal{E}$  will lead to a redistribution of the likelihood of wave heights (see figure 1), boosting the chances of encountering waves with  $\alpha \geq 0.8$  and decreasing the chances for ordinary sized waves  $0 < \alpha < 0.8$ . Due to the vertical asymmetry  $\mathfrak{S}$  between wave crests and troughs, the repartitioning of probability is further enhanced as the wave spectrum is broadened and waves become more nonlinear and asymmetric. In practice, the impact of the energy repartitioning is negligible on the bulk ( $0 < \alpha < 0.5$ ) of the exceedance probability but significant for large and rogue waves ( $\alpha \gtrsim 1$ ).

### III. ANALYTICAL SLOPE EFFECT

While our previous work focused on steep slopes, we now investigate the effect of an arbitrary finite slope. In shallow depths ( $H_s = h_0$ ) [42], a constant slope  $\nabla h$  implies an evolution of  $h(x)$  and an associated slope-induced set-down ( $\langle \zeta \rangle < 0$ ) or set-up ( $\langle \zeta \rangle > 0$ ) effect (see figure 2) that affects the energy (and hence the rogue wave probability) [37] [43] on top of the effect previously investigated

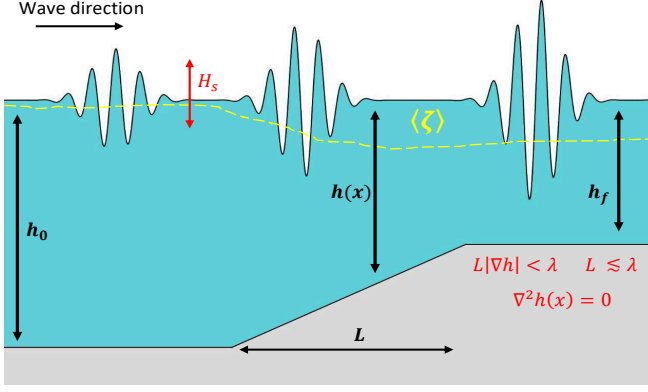


FIG. 2: Extreme wave amplification due to a shoal and assumptions for the solution. Within  $x \in [0, L]$  the depth evolves as  $h(x) = h_0 + x\nabla h$  with slope  $\nabla h = (h_f - h_0)/L$ . Note that the diagram is not to scale.

in Mendes *et al.* [29]:

$$\begin{aligned} \mathcal{E}_p + \mathcal{E}_k = & \frac{1}{2\lambda} \int_0^\lambda \left\{ \left[ \zeta(x, t) + h(x) + \langle \zeta \rangle \right]^2 - h^2(x) \right\} dx \\ & + \frac{1}{2\lambda g} \int_0^\lambda \int_{-h(x)}^\zeta \left[ \left( \frac{\partial \Phi}{\partial x} \right)^2 + \left( \frac{\partial \Phi}{\partial z} \right)^2 \right] dz dx, \quad (8) \end{aligned}$$

where  $(\mathcal{E}_p, \mathcal{E}_k)$  are the potential and kinetic energies and we assume  $L|\nabla h|/\lambda \lesssim 1$ . The slope  $\nabla h$  affects physical variables such as  $\nabla \lambda$ , and the integrand of  $\mathcal{E}_k$  will be modified by  $(x\nabla k_p/k_p)^2$  due to non-negligible derivatives from  $(\partial \Phi/\partial x)^2$ , and we find in the limit of numerous spectral components [44]:

$$\mathcal{E}_k \approx \sum_m \frac{\Omega_m^2}{4} \cdot \frac{\sinh(2mkh)}{2mgk}, \quad \forall (\nabla \lambda)^2 \lesssim 3. \quad (9)$$

On the other hand, the potential energy reads:

$$\begin{aligned} \mathcal{E}_p \equiv \mathcal{E}_{p1} + \mathcal{E}_{p2} = & \frac{1}{2\lambda} \int_0^\lambda \left[ \zeta^2(x, t) + 2h(x)\zeta(x, t) \right] dx \\ & + \frac{1}{2\lambda} \int_0^\lambda \left[ \langle \zeta \rangle^2 + 2\langle \zeta \rangle \zeta(x, t) + 2\langle \zeta \rangle h(x) \right] dx. \quad (10) \end{aligned}$$

Due to periodicity, integrals of  $\zeta\langle \zeta \rangle$  and  $\zeta h$  vanish [45]. Moreover,  $\mathcal{E}_{p1} + \mathcal{E}_k$  recovers eq. (4) while the slope effect on the energy is restricted to  $\mathcal{E}_{p2}$ :

$$\mathcal{E}_{p2} = \frac{8}{\mathfrak{S}^2 h_0^2} \cdot \frac{1}{\lambda} \int_0^\lambda \left[ \langle \zeta \rangle^2 + 2\langle \zeta \rangle h(x) \right] dx, \quad (11)$$

where we have used  $a = \mathfrak{S}H/2 = \mathfrak{S}H_s/2\sqrt{2}$ . Because the set-down is very small even in shallow water  $|\langle \zeta \rangle|/h_0 < 1/20$  [46, 47], we find to leading order:

$$\mathcal{E}_{p2} \approx \frac{16\langle \zeta \rangle}{\mathfrak{S}^2 h_0} \int_0^\lambda \left[ 1 + \frac{x\nabla h}{h_0} \right] \frac{dx}{\lambda} = \frac{16}{\mathfrak{S}^2} \left( \frac{\langle \zeta \rangle}{h_0} \right)_{\nabla h} \left[ 1 + \tilde{\nabla} h \right], \quad (12)$$

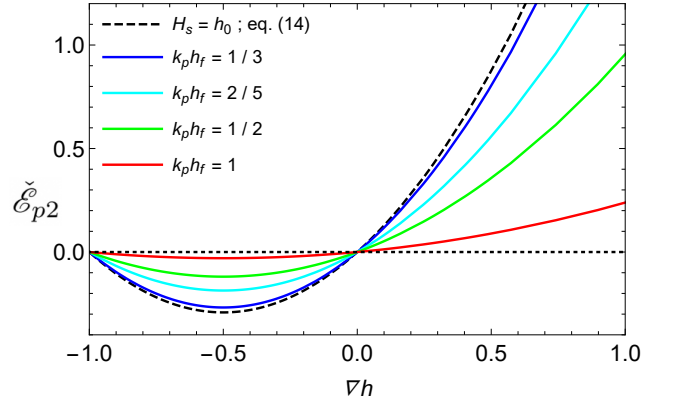


FIG. 3: Computation of  $\tilde{\mathcal{E}}_{p2}$  from eqs. (15) (solid) and eq. (14) (dashed) for an initial depth  $k_p h_0 = \pi$  and  $\varepsilon = 1/7$ .

where  $\tilde{\nabla} h \equiv \pi\nabla h/kh_0$  and  $f_{\nabla h}$  denotes  $f$  being a function of  $\nabla h$ . An increase or decrease of the rogue wave probability is controlled by the magnitude and sign of  $\langle \zeta \rangle$  for mild slopes, which depends on the slope [48]. For steep slopes, the term in brackets saturates the increase in probability in the case of a shoal. Following common practice, we linearize the set-down at the region near but prior to the wave breaking zone [46, 47] [49]:

$$\nabla \langle \zeta \rangle \approx \frac{\nabla h}{5} \left[ 1 + \frac{8h^2}{3H_s^2} \right]^{-1} \cdot \left( \frac{\nabla \langle \zeta \rangle}{\nabla h} \right)_{\frac{H_s}{h} \ll 1} \approx \frac{1}{5} \cdot \frac{3H_s^2}{8h^2}. \quad (13)$$

Since we consider the region prior to wave breaking, the associated set-up does not develop. However, the deshoal induces another form of set-up of smaller magnitude commonly called piling up [50, 51]. Integrating eq. (13) over a wavelength and plugging into eq. (12), we find for broad-banded waves:

$$\tilde{\mathcal{E}}_{p2} \approx \frac{96}{55\mathfrak{S}^2} \frac{\pi\nabla h}{k_p h_0} \left[ 1 + \frac{\pi\nabla h}{k_p h_0} \right] \approx \frac{6}{5} \tilde{\nabla} h \left( 1 + \tilde{\nabla} h \right). \quad (14)$$

However, the effect of depth change on the energy density ratio is expected to vanish in deep water, as the exchange of momentum encoded in the radiation stress becomes negligible [39]. Therefore, we seek a parameterization that generalizes the slope effect to intermediate depths, and the energy ratio shall evolve towards intermediate depths in the same way as eq. (13). That is to say,  $\tilde{\mathcal{E}}_{p2}(H_s \ll h_0)/\tilde{\mathcal{E}}_{p2}(H_s = h_0)$  is identical to  $(\nabla \langle \zeta \rangle/\nabla h)_{H_s \ll h}/(\nabla \langle \zeta \rangle/\nabla h)_{H_s = h}$ . We multiply both numerator and denominator of eq. (13) by  $k_p^2$  and convert the numerator peak wavelength to zero-crossing wavelength  $k_p H_s \approx (\pi/\mathfrak{S}\sqrt{2})\varepsilon$  [29] (see figure 3):

$$\tilde{\mathcal{E}}_{p2}(k_p h) \approx \frac{\pi\nabla h}{k_p h_0} \left[ 1 + \frac{\pi\nabla h}{k_p h_0} \right] \times \frac{6\pi^2}{5\mathfrak{S}^4} \frac{\varepsilon^2}{(k_p h)^2}. \quad (15)$$

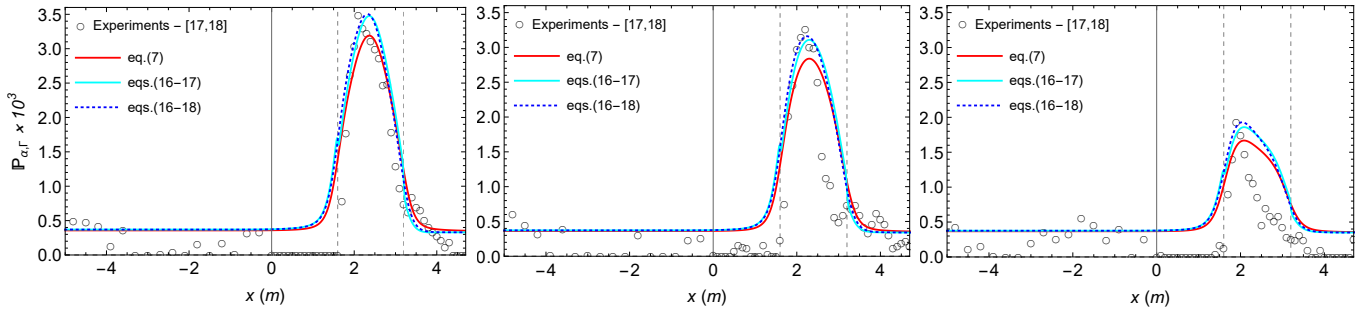


FIG. 4: Exceedance probability evolution over a bar from eq. (17) versus data (hollow circles) [17]. The probability evolution has been computed from eq. (7) as in Mendes *et al.* [29] (solid red) and the slope-dependent counterpart in eq. (16) without (cyan) and with (dotted blue) smoothing of the bar geometry ( $\vartheta = 3$ ) from eq. (18). Note that the experiments of Trulsen *et al.* [18] lie within all assumptions leading to eq. (16).

Plugging eq. (15) and  $\check{\mathcal{E}}_{p1} + \check{\mathcal{E}}_k$  into eq. (3) leads to a generalized finite-depth slope-dependent  $\Gamma_{\nabla h}$ :

$$\Gamma_{\nabla h} = \frac{\langle \zeta^2 \rangle_t(x)}{\mathcal{E}_{p1}(x) + \mathcal{E}_{p2}(x) + \mathcal{E}_k(x)}, \quad (16)$$

$$= \frac{1 + \frac{\pi^2 \varepsilon^2 \mathfrak{S}^2 \bar{\chi}_1}{16}}{1 + \frac{\pi^2 \varepsilon^2 \mathfrak{S}^2 (\bar{\chi}_1 + \chi_1)}{32} + \frac{\pi \nabla h}{k_p h_0} \left[ 1 + \frac{\pi \nabla h}{k_p h_0} \right] \frac{6\pi^2 \varepsilon^2}{5\mathfrak{S}^4 (k_p h)^2}}.$$

Note that the effect of the set-down on the numerator is negligible [52]. Eq. (16) indicates that increasing the slope of a mild shoaling  $\nabla h < 0$  will also increase the rogue wave probability. Furthermore,  $\Gamma_{\nabla h}$  will saturate when we reach  $\nabla h_{(s)} = -k_p h_0 / 2\pi$ , and cancel out when  $\nabla h_{(c)} = -k_p h_0 / \pi$ , see figure 3. On the other hand, at de-shoaling zones ( $\nabla h > 0$ ) following a shoal, eq. (16) describes a monotonic decrease in rogue wave probability due to the piling up when the down slope is increased because the term  $\check{\mathcal{E}}_{p2}$  increases monotonically.

Previous theories disregarding the slope were restricted to the range  $|\nabla h| \geq 1/20$ . In contrast, the validity of our derivation is only limited by the assumption  $L|\nabla h|/\lambda \lesssim 1$  in eq. (10), which is why the energy ratio correction diverges  $|\check{\mathcal{E}}_{p2}| \rightarrow \infty$  for  $\pi|\nabla h|/k_p h_0 \gg 1$ . Thus, the shoal case of our model is valid for  $0 < |\nabla h| \lesssim k_p h_0 / \pi$ . Nonetheless, this range covers realistic conditions in the ocean, where shoaling geometries with the highest slope steepness do not exceed  $|\nabla h| \approx 1$  [53, 54]. While only  $< 1\%$  of slopes over ocean cross-sections exceed  $|\nabla h| \approx 1$ , the typical mean slopes are  $< 1/10$  [55].

We compute the slope effect on  $\Gamma_{\nabla h}$  for experiments of Raustøl [17] and Trulsen *et al.* [18], plotted in figure 4. For this purpose, the evolution of exceedance probability  $\mathbb{P}_\alpha \equiv \mathbb{P}(H > \alpha H_s)$  over a shoal is described as [29]:

$$\ln \left( \frac{\mathbb{P}_{\alpha, \Gamma, \nabla h}}{\mathbb{P}_\alpha} \right) = 2\alpha^2 \left( 1 - \frac{1}{\mathfrak{S}^2 \Gamma_{\nabla h}} \right). \quad (17)$$

At the peak locations and in the de-shoaling zones (figure 4), we improve (cyan curve) the agreement with experimental data as compared with the model disregarding the slope (red curve), although the discrepancy in exceedance

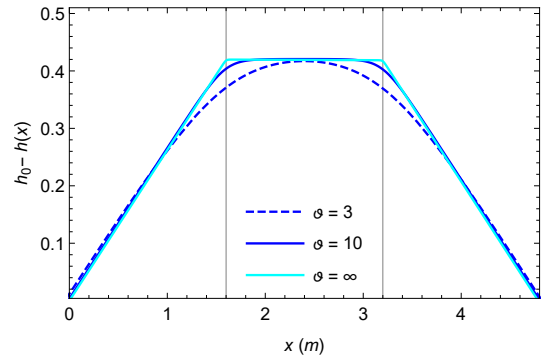


FIG. 5: Bathymetry smoothing of the bar in Trulsen *et al.* [18] generated from the integral of the slope function  $\nabla h(x)$  with finite parameter  $\vartheta$  as compared to the experimental bathymetry with  $\vartheta = \infty$ .

probability between models displayed in all panels of figure 4 does not exceed 8% at the location of maximum amplification of the exceedance probability. This surprisingly good fidelity of the model disregarding slope is due to the saturation evidenced in eq. (16). Indeed, the experimental slope  $\nabla h \approx -0.26$  happened to be close to saturation at  $(\nabla h)_{(s)} = -(9/5) \cdot (1/2\pi) \approx -0.29$ . Although our model implementing the exact slope effect is more accurate than the steep slope approximation of Mendes *et al.* [29], the experiments demonstrate that as long as the shoaling slope is near saturation the simpler model of Mendes *et al.* [29] is already very accurate. This provides a physical interpretation for the success of theories based on a step [24, 26, 29] in describing steep slope configurations.

However, we also checked the applicability of our model to real ocean slopes which vary smoothly and continuously, whereas the bar in the considered experiment features sharp edges. To that purpose, we numerically smoothed the edges of the bar employing logistic functions with parameter  $\vartheta$ :

$$\frac{\nabla h(x)}{|\nabla h|} = \frac{1}{1 + e^{-\vartheta(x-L)}} \left( 1 + \frac{1}{1 + e^{-\vartheta(x-2L)}} \right) - 1. \quad (18)$$

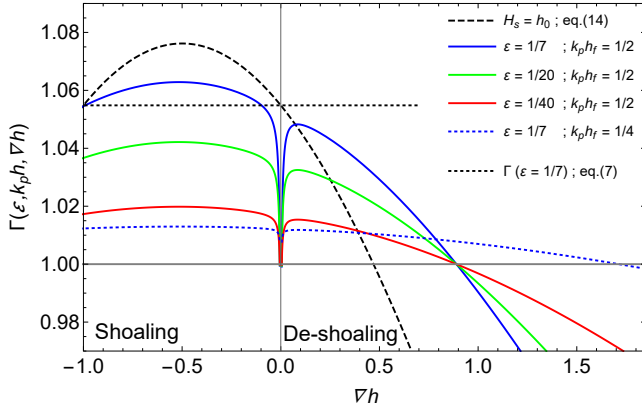


FIG. 6: Computation of  $\Gamma_{\nabla h}$  from eqs. (29) (solid), eq. (14) (dashed) and Mendes *et al.* [29] (dotted), for an initial depth  $k_p h_0 = \pi$ .

Therefore, we investigated the effect of using the smoothed slope function on the exceedance probability evolution. We verified that the amplification of the exceedance probability displayed in figure 4 with smoothed shoal edges (dotted curve) marginally deviates from the exact  $\nabla h$  (cyan curve) for  $\vartheta \gtrsim 3$  corresponding to a bell-shaped bar (see figure 5), and is indiscernible from the sharp edges when  $\vartheta \geq 10$ . This insensitivity to curvature ensures the applicability to real shapes in the ocean.

Finding the excursion of the slope function in the region of  $\Gamma_{\nabla h}(\nabla h \rightarrow 0) = 1$  would require the analytical evolution  $\varepsilon(\nabla h)$ , that is unavailable [56–60]. Therefore, we perform a parameterization. A residue  $B(k_p h, \nabla h)$  relevant only for very mild slopes is introduced:

$$\check{\mathcal{E}}_{p2}(k_p h) \approx \frac{\pi \nabla h}{k_p h_0} \left[ 1 + \frac{\pi \nabla h}{k_p h_0} \right] \frac{6\pi^2 \varepsilon^2}{5\mathfrak{S}^4(k_p h)^2} + B(k_p h, \nabla h), \quad (19)$$

noting that  $\lim_{\nabla h \rightarrow 0} \check{\mathcal{E}}_{p2} = \lim_{\nabla h \rightarrow 0} B$  and

$$\lim_{\nabla h \rightarrow 0} \Gamma_{\nabla h} = \frac{1 + \frac{\pi^2 \varepsilon^2 \mathfrak{S}^2}{16} \tilde{\chi}_1}{1 + \frac{\pi^2 \varepsilon^2 \mathfrak{S}^2}{32} (\tilde{\chi}_1 + \chi_1) + B(k_p h, \nabla h = 0)} = 1. \quad (20)$$

Denoting  $|\nabla h|_- \ll 1/20$  and  $|\nabla h|_+ > k_p h_0$  as the slopes minimizing and maximizing the slope effect on the exceedance probability, eq. (20) imposes:

$$B(|\nabla h|_-) = \frac{\pi^2 \varepsilon^2 \mathfrak{S}^2}{32} (\tilde{\chi}_1 - \chi_1) > 0. \quad (21)$$

The flat bottom boundary condition also requires [61]:

$$\lim_{\nabla h \rightarrow |\nabla h|_-} \frac{\partial \Gamma_{\nabla h}}{\partial |\nabla h|} > 0 \quad \therefore \quad \lim_{\nabla h \rightarrow |\nabla h|_-} \frac{\partial B}{\partial |\nabla h|} < 0, \quad (22)$$

imposing the form  $B(k_p h, \nabla h) = B_0(k_p h) |\nabla h|^{-n}$  [62]. Causality and neglecting reflection effects on  $\Gamma$  lead to:

$$\lim_{k_p h \rightarrow k_p h_0} \Gamma(\varepsilon, |\nabla h|_+) = \lim_{k_p h \rightarrow k_p h_0} \Gamma(\varepsilon, |\nabla h|_-). \quad (23)$$

Applying the general form of  $B(k_p h, \nabla h)$  to eqs. (19,23) results in:

$$\frac{6\pi^3 \varepsilon_0^2 |\nabla h|_+}{5\mathfrak{S}^4(k_p h_0)^3} \left[ 1 \pm \frac{\pi |\nabla h|_+}{k_p h_0} \right] = \pm B(k_p h_0, |\nabla h|_-), \quad (24)$$

with  $\pm$  denoting de-shoaling and shoaling, respectively. To leading order in  $|\nabla h|_+ / |\nabla h|_- \sim 10^{-2}$  we obtain:

$$B(k_p h_0, \nabla h) \approx \frac{6\pi^2}{25\mathfrak{S}^4} \frac{\pi^2 \varepsilon_0^2}{2000(k_p h_0)^4} \frac{|\nabla h|_-^{n-2}}{|\nabla h|^n}. \quad (25)$$

By definition,  $|\nabla h|_-$  corresponds to the limit in eq. (20). Having  $6\pi^2/25\mathfrak{S}^4 \approx 1$  [13, 29], we equate eqs. (21,25):

$$|\nabla h|_- \approx \frac{\varepsilon_0}{\varepsilon} \frac{1}{\sqrt{90(k_p h_0)^4 (\tilde{\chi}_1 - \chi_1)}}, \quad (26)$$

so that  $|\nabla h|_- \approx 1/90$  for  $k_p h \in [0.5, 1.5]$ , experimentally observed in Katsardi *et al.* [63]. At the depth corresponding to the maximum amplification ( $k_p h \approx 1/2$ ) eq. (21) results in  $B(|\nabla h|_-) \approx 5\pi^2 \varepsilon^2$ . Since the slope effect loses importance for  $|\nabla h| > 1/20$ , the growth becomes  $(\partial B / \partial |\nabla h|)_{|\nabla h|_-} > -120\pi^2 \varepsilon^2$ . Then, the derivative of eq. (25) imposes  $n \approx \pi^2/12 \sim 1$ :

$$B(k_p h, \nabla h) \approx \frac{\pi^2}{25(k_p h_0)^2} \frac{\varepsilon^2}{(k_p h)^2 |\nabla h|}. \quad (27)$$

The intermediate depth energy ratio reads:

$$\check{\mathcal{E}}_{p2} \approx \frac{5\varepsilon^2}{(k_p h)^2} \left\{ \frac{\pi \nabla h}{k_p h_0} \left[ 1 + \frac{\pi \nabla h}{k_p h_0} \right] + \frac{\pi^2}{125(k_p h_0)^2 |\nabla h|} \right\}. \quad (28)$$

Plugging eq. (28) into eq. (16) results in (figure 6),

$$\Gamma(k_p h, \varepsilon, \nabla h) = \frac{1 + \frac{\pi^2 \varepsilon^2 \mathfrak{S}^2}{16} \tilde{\chi}_1}{1 + \frac{\pi^2 \varepsilon^2 \mathfrak{S}^2}{32} (\tilde{\chi}_1 + \chi_1) + \frac{5\varepsilon^2}{(k_p h)^2} \left\{ \frac{\pi \nabla h}{k_p h_0} \left[ 1 + \frac{\pi \nabla h}{k_p h_0} \right] + \frac{\pi^2}{125(k_p h_0)^2 |\nabla h|} \right\}}. \quad (29)$$

The cancelling effect of  $B(k_p h, \nabla h)$  on the pre-shoal flat bottom  $\Gamma$  clearly appears around  $\nabla h = 0$  in figure 6.

However, when  $k_p h \rightarrow 0$  the trigonometric coefficients  $(\chi_1, \tilde{\chi}_1) \rightarrow \infty$  grow much faster than  $\check{\mathcal{E}}_{p2}$ , and  $\Gamma$  no longer

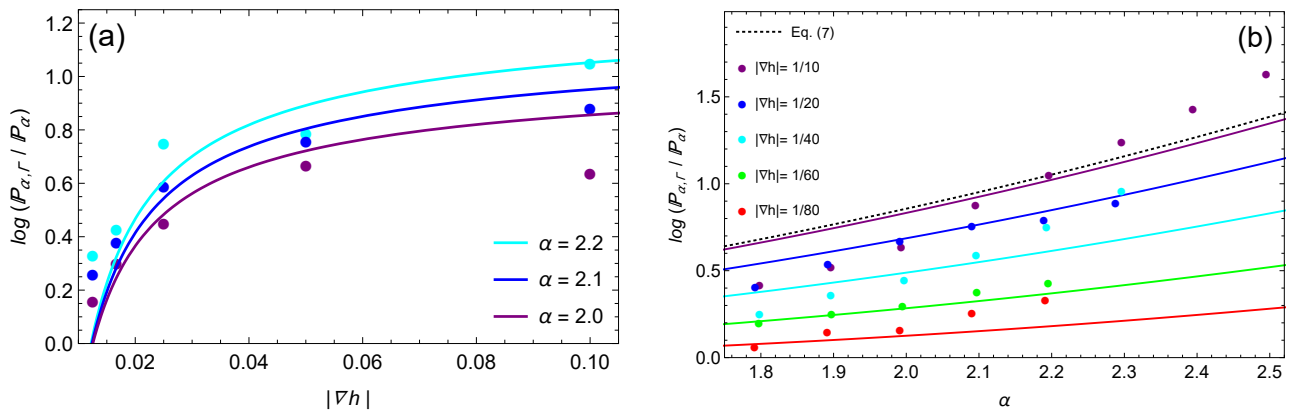


FIG. 7: Ratio of exceedance probabilities (relative to the Rayleigh distribution) as a function of (a) slope  $\nabla h$  and (b) normalized heights  $\alpha = H/H_s$  reported from Zheng *et al.* [33]. Dots display numerical data at  $k_p h = 0.7$  while our model of eq. (7) is shown in dotted line and eq. (29) in solid lines.

depends on  $\nabla h$ . This slow dependence on the slope in shallow waters (see the blue dotted curve in figure 6) has been observed in Doleman [64], which carrying experiments at  $k_p h_0 \approx 0.38$  found the evolution of the kurtosis for a step ( $|\nabla h| = \infty$ ) and a slope of  $|\nabla h| = 0.05$  to be identical. Our model explains this phenomenon with the proximity of the slope to the saturation point  $|\nabla h|_{(s)} = k_p h_0 / 2\pi \approx 0.06$ .

Experiments with wide ranges of slopes, i.e. with length  $L \sim \lambda$  and water depth  $\pi/10 \lesssim k_p h \lesssim \pi/2$ , are not available to date because mild slopes usually require lengths exceeding wave tank dimensions or wave frequencies must be too high for the given dimensions. Hence, in the absence of experiments with broad ranges for slopes, steepness and water depth, we assess our theory against the numerical results of Zheng *et al.* [33], describing how the probability of the envelope [65] is affected by increasing the slope steepness. In figure 13 of Zheng *et al.* [33] the shoal increased the exceedance probability for rogue waves as soon as  $|\nabla h| = 1/80$ , with a saturation of this effect for slopes steeper than  $|\nabla h| \gtrsim 1/10$  (the details of physical variables of the performed simulations C1-C8 are found on table II in Zheng *et al.* [33]). We apply the same conditions to the slope-dependent non-homogeneous correction of eqs. (7), (16), (29) and (17) and compare the maximum amplification ( $\varepsilon = 1/16$ ) of the exceedance probability (figure 7). Our model reproduces well the exceedance probability for rogue waves ( $\alpha > 2$ ) and its saturation for steep slopes (figure 7a) or for large waves  $\alpha \geq 1.75$  with fixed slope as shown in figure 7b. Furthermore, we recover our previous model [29] for the steepest slopes (see dotted line in figure 7b).

#### IV. DISCUSSION

The slope effect on the exceedance probability can be interpreted as a second redistribution of the wave statistics, on top of that induced by the depth change. In

the presence of a strong departure from a zero-mean water level due to a set-down/set-up the potential energy density is affected by a slope-induced correction  $\mathcal{E}_{p2}$ . In the case of a shoal, such energy disturbance decreases the total potential energy as compared to linear homogeneous waves, thereby increasing the effect of the energy redistribution ( $\Gamma_{\nabla h} > \Gamma$ ). Similarly, a set-up induced by wave-breaking would cause the total potential energy to increase, and so we would observe the opposite effect by decreasing the exceedance probability because of  $\Gamma_{\nabla h} < \Gamma$ . This means that the depth change has the leading order in amplifying the exceedance probability over a shoal when the slope steepness does not vanish ( $|\nabla h| \rightarrow 0$ ), while the slope modulates the energy redistribution due to this depth change.

The saturation of the slope effect can be understood as a combination of the effect of lowering the mean water level as a function of the slope and of the pace of the depth transition itself. The secondary term in brackets of eq. (14) is equivalent to  $\langle h(x)/h_0 \rangle$ . A continuous steep slope  $|\nabla h| \rightarrow \infty$  implies  $\langle h(x)/h_0 \rangle \rightarrow 0$  over the wave relaxation region following the start of the shoal. Indeed, over this region the mean depth converges to the shallower depth. In the meantime, a very steep slope will quickly increase the set-down. Nevertheless, the fast increase in the set-down is balanced by the fast decrease in mean depth, therefore creating the observed saturation of their product, namely  $\mathcal{E}_{p2}$ . In other words, the response of the set-down to the steep slope transition past the saturation point is slower than the depth transition itself and has no time to develop. Conversely, in the de-shoaling zone the faster increase of the set-up due to steeper slopes is not balanced by the depth transition, as the mean depth will increase rather than decrease.

Our framework poses a clear unifying picture for wave statistics and energetics transitioning from deep to shallow waters: (i) waves in deep water will not have their energy affected by the slope and tend to follow Gaussian statistics, (ii) in intermediate water the wave energy

density will be redistributed due to depth effects on the steepness, vertical asymmetry and mean water level, ultimately increasing rogue wave likelihoods, (iii) in shallow water the effects on steepness and vertical asymmetry still exist, but the quick divergence of the superharmonics halts the energy redistribution while the set-up inverts the latter. Therefore, in the absence of any ocean process besides shoaling, we unify within a single physical mechanism the seemingly contradictory results of Longuet-Higgins [41] in deep water, Trulsen *et al.* [18] in intermediate water and Glukhovskii [19] in shallow water.

## V. CONCLUSIONS

We have for the first time obtained an analytical dependence of the wave height exceedance probability on  $\nabla h$ . It widely extends the approach developed for steps and unifies the theories for wave statistics in deep, intermediate and shallow waters within a dynamical evolution. The unified framework is laid out as bathymetry effects on the energy partition between waves of different heights, and therefore the probability distribution, by considering the specific effects of the slope beyond the sole bathymetry change. Models that do not take finite slopes into account are nonetheless capable of reproducing well the wave statistics of steep slopes [24, 26, 29]. We explain this equivalency between a step and steep slopes with the saturation effect as evidenced from eq. (16). When slopes become too steep and we reach saturation,

the success of these models can be interpreted as the result of the slope effect being fully encoded in the change of both steepness and depth. Although our model does not cover the limiting case of a step *per se*, both steep and mild bathymetric profiles in the ocean are well covered by the model range of validity. Furthermore, our range of validity is consistent with small reflection effect due to a non-diverging surf similarity. Qualitatively, our theory points to three major consequences. Firstly, making a mild slope steeper increases the probability of large wave heights in shoaling zones, and decreases it in de-shoaling zones following a shoal. Secondly, in very shallow water the slope effect already saturates even for mild slopes, while in intermediate waters the saturation point is harder to attain. Thirdly, we reconcile the transient increase of rogue wave probability over a shoal with lower probabilities in shallow water. We have quantitatively validated our model against the numerical results of Zheng *et al.* [33] and the experiments of Raustøl [17] for the exceedance probability of wave heights, obtaining good agreement. Finally, the unification of rogue wave formation mechanisms within the present framework should be possible, provided future work addresses the out-of-equilibrium ocean processes driving non-Gaussian statistics over a flat bottom, such as opposing currents and crossing seas.

## VI. ACKNOWLEDGMENTS

S.M. and J.K. were supported by the Swiss National Science Foundation under grant 200020-175697. We thank Maura Brunetti for fruitful discussions.

- 
- [1] M. Onorato, S. Residori, U. Bortolozzo, A. Montina, and F. Arecchi, Rogue waves and their generating mechanisms in different physical contexts, *Phys. Rep.* **528**, 47 (2013).
  - [2] R. Sabry, W. Moslem, and P. Shukla, Freak waves in white dwarfs and magnetars, *Phys. Plasmas* **19** (2012).
  - [3] R. Sabry, Freak waves in saturn's magnetosphere, *Astrophys. Space Sci.* **355**, 33 (2014).
  - [4] D. Solli, C. Ropers, P. Koonath, and B. Jalali, Optical rogue waves, *Nature* **450**, 1054 (2007).
  - [5] B. Kibler, J. Fatome, C. Finot, G. Millot, F. Dias, G. Genty, N. Akhmediev, and J. Dudley, The peregrine soliton in nonlinear fibre optics, *Nat. Phys.* **6**, 790 (2010).
  - [6] V. Efimov, A. Ganshin, G. Kolmakov, P. McClintock, and L. Mezhov-Deglin, Rogue waves in superfluid helium, *Eur. Phys. J. Spec. Top.* **185**, 181 (2010).
  - [7] L. Wen, L. Li, Z. Li, S. Song, X. Zhang, and W. Liu, Matter rogue wave in bose-einstein condensates with attractive atomic interaction, *Eur. Phys. J. D* **64**, 473 (2011).
  - [8] P. Liu, A chronology of freak wave encounters, *Geofizika* **24**, 57 (2007).
  - [9] E. Didenkulova, Catalogue of rogue waves occurred in the world ocean from 2011 to 2018 reported by mass media sources, *Ocean and Coastal Management* **188** (2020).
  - [10] T. B. Benjamin and J. E. Feir, The disintegration of wave trains on deep water part 1. theory, *Journal of Fluid Mechanics* **27**, 417 (1967).
  - [11] P. Boccotti, *Wave mechanics and wave loads on marine structures*, Elsevier (2014).
  - [12] I. Karmpadakis, C. Swan, and M. Christou, Assessment of wave height distributions using an extensive field database, *Coastal Eng.* **157** (2020).
  - [13] S. Mendes, A. Scotti, and P. Stansell, On the physical constraints for the exceeding probability of deep water rogue waves, *Appl. Ocean Res.* **108**, 102402 (2021).
  - [14] S. Mendes and A. Scotti, The rayleigh-haring-tayfun distribution of wave heights in deep water, *Applied Ocean Research* **113**, 102739 (2021).
  - [15] I. Karmpadakis, C. Swan, and M. Christou, A new wave height distribution for intermediate and shallow water depths, *Coastal Engineering* **175**, 104130 (2022).
  - [16] K. Trulsen, H. Zeng, and O. Gramstad, Laboratory evidence of freak waves provoked by non-uniform bathymetry, *Phys. Fluids* **24** (2012).
  - [17] A. Raustøl, *Freake bølger over variabelt dyp*, Master's thesis, University of Oslo (2014).
  - [18] K. Trulsen, A. Raustøl, S. Jorde, and L. Rye, Extreme wave statistics of long-crested irregular waves over a shoal, *J. Fluid Mech.* **882** (2020).

- [19] B. Glukhovskii, Investigation of sea wind waves (in russian), Gidrometeoizdat (1966).
- [20] Y. Wu, D. Randell, M. Christou, K. Ewans, and P. Jonathan, On the distribution of wave height in shallow water, *Coastal Eng.* **111**, 39 (2016).
- [21] S. Mendes and A. Scotti, Rogue wave statistics in (2+1) gaussian seas i: Narrow-banded distribution, *Appl. Ocean Res.* **99**, 102043 (2020).
- [22] C. Lawrence, K. Trulsen, and O. Gramstad, Extreme wave statistics of surface elevation and velocity field of gravity waves over a two-dimensional bathymetry, *J. Fluid Mech.* **939**, A41 (2022).
- [23] Y. Li, Y. Zheng, Z. Lin, T. A. Adcock, and T. Van Den Bremer, Surface wavepackets subject to an abrupt depth change. part 1: Second-order theory, *J. Fluid Mech.* **915**, A71 (2021).
- [24] Y. Li, S. Draycott, Y. Zheng, Z. Lin, T. Adcock, and T. Van Den Bremer, Why rogue waves occur atop abrupt depth transitions, *Journal of Fluid Mechanics* **919**, R5 (2021).
- [25] A. Majda, M. Moore, and D. Qi, Statistical dynamical model to predict extreme events and anomalous features in shallow water waves with abrupt depth change, *Proceedings of the National Academy of Sciences of the United States of America* **116**, 3982 (2019).
- [26] N. Moore, C. Bolles, A. Majda, and D. Qi, Anomalous waves triggered by abrupt depth changes: Laboratory experiments and truncated kdv statistical mechanics, *Journal of Nonlinear Science* **30**, 3235 (2020).
- [27] M. Donelan, W. Drennan, and A. Magnusson, Nonstationary analysis of the directional properties of propagating waves, *Journal of Physical Oceanography* **26**, 1901 (1996).
- [28] K. Trulsen, Rogue waves in the ocean, the role of modulational instability, and abrupt changes of environmental conditions that can provoke non equilibrium wave dynamics, in: *The Ocean in Motion: Circulation, Waves, Polar Oceanography* (2018).
- [29] S. Mendes, A. Scotti, M. Brunetti, and J. Kasparian, Non-homogeneous model of rogue wave probability evolution over a shoal, *J. Fluid Mech.* **939**, A25 (2022).
- [30] G. Ducrozet, M. Abdolahpour, F. Nelli, and A. Toffoli, Predicting the occurrence of rogue waves in the presence of opposing currents with a high-order spectral method, *Physical Review Fluids* **6**, 064803 (2021).
- [31] D. Andrade, R. Stuhlmeier, and M. Stiassnie, Freak waves caused by reflection, *Coastal Eng.* **170**, 104004 (2021).
- [32] O. Gramstad, H. Zeng, K. Trulsen, and G. Pedersen, Freak waves in weakly nonlinear unidirectional wave trains over a sloping bottom in shallow water, *Physics of Fluids* **25** (2013).
- [33] Y. Zheng, Z. Lin, Y. Li, T. Adcock, Y. Li, and T. Van Den Bremer, Fully nonlinear simulations of unidirectional extreme waves provoked by strong depth transitions: The effect of slope, *Phys. Rev. Fluids* **5** (2020).
- [34] C. Lawrence, K. Trulsen, and O. Gramstad, Statistical properties of wave kinematics in long-crested irregular waves propagating over non-uniform bathymetry, *Physics of Fluids* **33** (2021).
- [35] M. S. Longuet-Higgins, Integral properties of periodic gravity waves of finite amplitude, *Proceedings of the Royal Society of London. A. Mathematical and Physical Sciences* **342**, 157 (1975).
- [36] G. B. Airy, Tides and waves, in *encyclopaedia metropolitana*, B.Fellows, London **122**, 241–396 (1845).
- [37] R. Dean and R. Dalrymple, *Water wave mechanics for engineers and scientists.*, World Scientific (1984).
- [38] M. B. Priestley, *Spectral analysis and time series: probability and mathematical statistics*, Vol. 1 (Academic Press, 1981).
- [39] L. H. Holthuijsen, *Waves in Oceanic and Coastal Waters* (Cambridge University Press, 2007).
- [40] The connection between  $(\Omega_m, \tilde{\Omega}_m)$  and the energies are detailed in equations 3.7-3.9 and B7-B9 of Mendes *et al.* [29].
- [41] M. Longuet-Higgins, On the statistical distribution of the heights of sea waves, *Journal of Marine Research* **11**, 245 (1952).
- [42] Surf-zone characteristics are reached when  $H_s \gtrsim h_0$ , see page 243 of Holthuijsen [39]. For shallow depths we refer to a narrow range of validity of between Stokes and KdV realms [66].
- [43] While the total energy  $\mathcal{E}$  changes over a shoal in part because of changes in  $c_g$ , in the absence of wave breaking the energy flux is constant  $\nabla(\mathcal{E} \cdot c_g) = 0$ . The radiation stress will continue to increase during the shoaling [67], thus producing a decrease in the mean water level from  $\langle \zeta \rangle = 0$  to  $\langle \zeta \rangle < 0$ . If the waves break, past the breaker line we have a positive set-up  $\langle \zeta \rangle > 0$ . However, Brevik [68] describes how other ocean processes can induce different types of set-down, such as wave group or current-induced. Although the wave group set-down over a flat bottom is accompanied by a small return flow [67, 69], the shoal-induced set-down induces a small forward flow [70, 71], and the conservation of mass near the beach or at the end of a wave tank works to cancel out this forward flow at the shoaling zone [71, 72].
- [44] Because  $\int_0^\lambda (x \nabla k_p / k_p)^2 dx / \lambda$  is equivalent to the integral  $\int_0^\lambda (x \nabla \lambda / \lambda)^2 dx / \lambda = (\nabla \lambda)^2 / 3$ .
- [45] The surface elevation can be decomposed into two parts  $\zeta^*(x, t) = \zeta(x, t) + \zeta_s(x, t)$ , where  $\zeta(x, t)$  denotes the zero-mean oscillatory motion and  $\zeta_s(x, t)$  the slope-induced set-down. However, Longuet-Higgins and Stewart [67] and subsequent literature did not derive the set-down  $\zeta_s(x, t)$  explicitly. The periodicity of the type of solutions for  $\zeta(x, t)$  in eq. (1) shows that its form must be  $\zeta_s(x, t) \sim \langle \zeta \rangle \cos^{2n}(m\phi)$  to fulfill  $\langle \zeta^*(x, t) \rangle = \langle \zeta_s(x, t) \rangle = \langle \zeta \rangle$ , with  $n \in \mathbb{N}$ . It is straightforward to show in the generalized case that  $\int_0^\lambda 2\zeta(x, t)\zeta_s(x, t)dx = \int_0^\lambda 2\zeta(x, t)\langle \zeta \rangle dx = 0$ . As long as  $\nabla^2 h = 0$  we have  $\int_0^\lambda \zeta(x, t)h(x)dx = 0$ . Hence, our implicit choice  $\zeta^*(x, t, n=0) = \zeta(x, t) + \langle \zeta \rangle$  in eq. (8) does not lead to any loss of generality.
- [46] A. Bowen, D. Inman, and V. Simmons, Wave ‘set-down’ and set-up, *Journal of Geophysical Research* **73**, 2569 (1968).
- [47] R. Guza and E. Thornton, Wave set-up on a natural beach., *Journal of Geophysical Research* **86**, 4133 – 4137 (1981).
- [48] U. T. Ehrenmark, Set-down computations over an arbitrarily inclined plane bed, *Journal of marine research* **52**, 983 (1994).
- [49] Although both set-down ( $\langle \zeta \rangle < 0$ ) and set-up ( $\langle \zeta \rangle > 0$ ) depend on the slope  $\nabla h$ , this complex dependence is either simplified or overlooked in the literature [73–77]. Indeed, the set-down/set-up are often related by a scaling of typically 1/5 [76, 78].

- [50] M. S. Longuet-Higgins, On the wave-induced difference in mean sea level between the two sides of a submerged breakwater, *J. mar. Res.* **25**, 148 (1967).
- [51] M. H. Diskin, M. L. Vajda, and I. Amir, Piling-up behind low and submerged permeable breakwaters, *Journal of the Waterways, Harbors and Coastal Engineering Division* **96**, 359 (1970).
- [52] Because  $2\langle\zeta^2\rangle/a^2 \rightarrow 2\langle(\zeta + \langle\zeta\rangle)^2\rangle/a^2$  is corrected by an integral of  $(4\langle\zeta\rangle/\mathfrak{S}h_0)^2 \sim \mathcal{O}(1/25\mathfrak{S}^2)$  and the vanishing integral of  $\zeta\langle\zeta\rangle$ , the former being much smaller than  $16\langle\zeta\rangle/\mathfrak{S}^2h_0 = \mathcal{O}(1/\mathfrak{S}^2)$  of eq. (12).
- [53] W. N. Seelig, Laboratory study of reef-lagoon system hydraulics, *Journal of Waterway, Port, Coastal and Ocean Engineering* **109**, 380 (1983).
- [54] D. J. W. Piper, Sedimentary processes: Deep water processes and deposits, in *Encyclopedia of Geology*, edited by R. C. Selley, L. R. M. Cocks, and I. R. Plimer (Elsevier, Oxford, 2005) pp. 641–649.
- [55] J. J. Becker and D. T. Sandwell, Global estimates of seafloor slope from single-beam ship soundings, *Journal of Geophysical Research: Oceans* **113** (2008).
- [56] P. S. Eagleson, Properties of shoaling waves by theory and experiment, *Eos, Transactions American Geophysical Union* **37**, 565 (1956).
- [57] N. Shuto, Nonlinear long waves in a channel of variable section, *Coastal Engineering in Japan* **17**, 1 (1974).
- [58] J. Walker and J. Headlam, Engineering approach to nonlinear wave shoaling, *Proceedings of the Coastal Engineering Conference* **1**, 523 (1983).
- [59] H.-M. Kweon and Y. Goda, A parametric model for random wave deformation by breaking on arbitrary beach profiles, *Coastal Engineering* 1996, 261 (1997).
- [60] V. Srineash and K. Murali, Wave shoaling over a submerged ramp: An experimental and numerical study, *Journal of Waterway, Port, Coastal and Ocean Engineering* **144** (2018).
- [61] The flat bottom boundary condition requires that  $\Gamma = 1$ . For the most part of  $\nabla h > 0$  we have a monotonically decreasing  $\Gamma_{\nabla h} < 1$ . However, according to eq. (16), for mild slopes  $\nabla h \ll 1/20$  in the de-shoaling zone we have  $1 < \Gamma_{\nabla h} < \Gamma$  with a sharp derivative  $\partial\Gamma_{\nabla h}/\partial|\nabla h| > 0$  for mild slopes as a corollary of the continuity of  $\hat{\mathcal{E}}_{p2}$ .
- [62] Having  $B = -B_0|\nabla h|^n$  we would not comply with eq. (21) because  $B$  would vanish instead of reaching relatively high positive values when  $|\nabla h| \ll 1/10$ .
- [63] V. Katsardi, L. de Lutio, and C. Swan, An experimental study of large waves in intermediate and shallow water depths. part i: Wave height and crest height statistics, *Coastal Eng.* **73**, 43 (2013).
- [64] M. W. Doleman, Rogue waves in the dutch north sea, Master’s thesis, TU Delft (2021).
- [65] The envelope is computed as  $R = \sqrt{\zeta^2 + \hat{\zeta}^2}$ , with  $\hat{\zeta}(x, t)$  the Hilbert transform of the surface elevation  $\zeta(x, t)$ . We may approximate  $R \approx H \approx 2a$  which leads to  $a/\sigma \approx 2\alpha = 2H/H_s$ , where  $\sigma^2 = \int_0^\infty S(\omega) d\omega$ .
- [66] B. Le Méhauté, An introduction to hydrodynamics and water waves, Springer (1976).
- [67] M. Longuet-Higgins and R. Stewart, Radiation stresses in water waves; a physical discussion, with applications, *Deep-Sea Research and Oceanographic Abstracts* **11**, 529 (1964).
- [68] I. Brevik, Remarks on set-down for wave groups and wave-current systems, *Coastal Engineering* **2**, 313 (1978).
- [69] M. Longuet-Higgins and R. Stewart, Radiation stress and mass transport in gravity waves, with application to ‘surf beats’, *Journal of Fluid Mechanics* **13**, 481 (1962).
- [70] M. S. Longuet-Higgins, Wave set-up, percolation and undertow in the surf zone, *Proceedings of the Royal Society of London. A. Mathematical and Physical Sciences* **390**, 283 (1983).
- [71] U. T. Ehrenmark, Eulerian mean current and stokes drift under non-breaking waves on a perfect fluid over a plane beach, *Fluid dynamics research* **18**, 117 (1996).
- [72] S. J. Lentz and M. R. Fewings, The wind-and wave-driven inner-shelf circulation, *Annual review of marine science* **4**, 317 (2012).
- [73] T. Saville, Experimental determination of wave set-up, in *Proc. 2nd Tech. Conf. on Hurricanes, Miami Beach, FL, 1961* (1961).
- [74] M. S. Longuet-Higgins and R. W. Stewart, A note on wave set-up, *Journal of Marine Research* **21**, 4 (1963).
- [75] R. A. Holman and A. Sallenger Jr, Setup and swash on a natural beach, *Journal of Geophysical Research: Oceans* **90**, 945 (1985).
- [76] S. R. Massel and M. R. Gourlay, On the modelling of wave breaking and set-up on coral reefs, *Coastal engineering* **39**, 1 (2000).
- [77] T.-W. Hsu, J. R.-C. Hsu, W.-K. Weng, S.-K. Wang, and S.-H. Ou, Wave setup and setdown generated by obliquely incident waves, *Coastal Engineering* **53**, 865 (2006).
- [78] J. A. Battjes, Computation of set-up, longshore currents, run-up and overtopping due to wind-generated waves, PhD Thesis, TU Delft (1974).